CFD Letters

Journal homepage: https://semarakilmu.com.my/journals/index.php/CFD_Letters/index
ISSN: 2180-1363

Radiative Hybrid Ferrofluid Flow Over a Permeable Shrinking Sheet in a Three-Dimensional System

Najiyah Safwa Khashi'ie[1,*], Iskandar Waini[1], Nur Syahirah Wahid[2], Norihan Md Arifin[2,3], Ioan Pop[4]

[1] Fakulti Teknologi Kejuruteraan Mekanikal dan Pembuatan, Universiti Teknikal Malaysia Melaka, Hang Tuah Jaya, 76100 Durian Tunggal, Melaka, Malaysia
[2] Department of Mathematics and Statistics, Faculty of Science, Universiti Putra Malaysia, 43400 UPM Serdang, Selangor, Malaysia
[3] Institute for Mathematical Research, Universiti Putra Malaysia, 43400 UPM Serdang, Selangor, Malaysia
[4] Department of Mathematics, Babeş-Bolyai University, R-400084 Cluj-Napoca, Romania

ARTICLE INFO

Article history:
Received 5 July 2022
Received in revised form 6 Sept. 2022
Accepted 10 September 2022
Available online 9 November 2022

Keywords:
Hybrid ferrofluid; magnetic field; radiation; shrinking sheet

ABSTRACT

Due to the significance of magnetic nanofluids in environmental and biomedical sectors, this study is designed to analyze the available solutions alongside with the flow and thermal behaviours of radiative hybrid ferrofluid flow in a three-dimensional system subjected to the shrinking surface. The case of Fe3O4-CoFe2O4/water is considered in this work. The initial procedure is conducted by reducing the complex model into a system of nonlinear differential equations using similarity transformation technique. The results are generated using the bvp4c package in the Matlab software and graphically presented. The existence of dual solutions leads to the treatment of stability analysis where the first solution is affirmed as the physical solution. Meanwhile, the impact of thermal radiation, magnetic field and suction are also observed for the distributions of thermal rate and skin friction coefficients. These distributions boost with the imposition of magnetic field and suction while a deterioration in thermal rate is observed with the rise of thermal radiation.

1. Introduction

Effective heat transmission is vital to improve the performance and compactness of heat exchanger devices and machines. Typically, cooling agents such as water and oil are employed in a variety of industrial processes such as power generation, chemical processing, and heating or cooling. Pure water generally is classified as Newtonian fluid while liquids like suspension solutions and lubricants are categorized as non-Newtonian fluid. Various non-Newtonian fluid models were numerically analyzed by these researchers [1-10]. Howbeit, as an initiative to improve the thermal properties of fluids, nanometre dimension particles (nanoparticles) were introduced, resulting in so-called nanofluids [11]. Nanofluids have been found to exhibit excellent stability and rheological characteristics, with much greater thermal conductivities and little penalty of pressure drop [12]. There are many advanced ideas and practical uses of nanofluids that provide unique heat

* *Corresponding author.*
E-mail address: najiyah@utem.edu.my

https://doi.org/10.37934/cfdl.14.11.921

transmission properties, such as solar collectors, medical devices, transformer applications, vehicle thermal management and electronic cooling [13-16].

Recently, ferrofluids or magnetic nanofluids, have piqued the interest of scientists owing to their paramagnetic features. Ferrofluids are stable colloidal suspensions of ultrafine single domain superparamagnetic nanoparticles mostly iron and its oxides such as magnetite or maghemite in polar or non-polar solvent [17]. The viscosity of ferrofluids is significant in optimising numerous commercial applications [18,19]. However, to further enhance the properties of nano/ferrofluid, hybrid nanofluid is later introduced. The suspensions of hybrid or composite nanoparticles in a solvent is found to exhibit higher thermal capability compared to the single suspension [20]. This was experimentally proven by Sundar *et al*., [21] where they found that by employing 0.3% of MWCN-Fe_3O_4/water, the Nusselt number and friction factor increased by 31% and 18%, respectively. Besides, a 21% Nusselt number enhancement was seen in another investigation for 0.009% of Fe_2O_3-TiO_2/water [22]. Mishra and Upreti [23] explored the mass and heat transfer properties of hybrid nanofluids namely Fe_3O_4-$CoFe_2O_4$ /water-ethylene glycol and Ag-MgO/water past a curved surface. The radiative flow of magnetic Fe_2O_3-CuO/ H_2O hybrid nanofluid over a porous extend/contract wedge was scrutinized by Izady *et al*., [24]. The magnetic parameter has shown that it has a favourable influence on the enhancement of heat transfer. Later, Elsaid and Abdel-wahed [25] solved the mixed convection of Fe_3O_4-Cu/H_2O hybrid nanofluid flow problem in a vertical channel with a uniform transverse magnetic field. The study towards Gr-Fe_3O_4/ H_2O hybrid nanofluid on a movable uniform surface is addressed by Khazayinejad and Nourazar [26] in elucidating the spatial fractional heat transfer. The elevation of temperature has been noticed when hybrid nanofluid was considered. There are several others interesting literature on hybrid nanofluid which can be referred here [27-32].

Researchers have found numerous applications for thermally radiative flow in industrial and space technology products. Thermal radiation, for example, is used in engineering technology, in the production of air conditioners, boilers, heaters, and crude oil refining. It is also employed in our hospitals for a variety of purposes including sterilisation of medical equipment, cancer, and tumour therapy. Rosseland [33] was the first to provide an equation for radiative heat flux that was used to examine flows with thermal radiation, and this expression was subsequently simplified by Sparrow and Cess [34]. For the latest investigation, Yaseen *et al*., [35] have studied the radiation effect on hybrid nanofluid slip flow past a movable surface for the forward and reverse flow. It has been shown in their research that radiation effect could augment the heat transmission. Conversely, different scenario was witnessed by Gumber *et al*., [36] in their investigation towards micropolar hybrid nanofluid flow past a vertical plate. The quadratic thermal radiation is later realized to procure greater Nusselt number compared to linear radiation [37]. Further readings on radiative hybrid nanofluid flow may be found in Refs. [38-40].

The effective heat transfer for different miniatures and technological processes continue to draw researchers to discover a concurrent solution to this challenge. This study is intended to analyze the thermal properties and fluid flow behaviour of radiative ferrofluid in a three-dimensional system subjected to a shrinking surface. The method of similarity transformation is utilised to simplify the governing model, which is then solved with the efficient bvp4c solver. The effect of physical characteristics such as suction and thermal radiation is explored, as well as the thermal augmentation capabilities of these ferrofluids.

2. Mathematical Formulation

We consider a three-dimensional flow of Fe_3O_4-$CoFe_2O_4$/water over a stretching/shrinking sheet where the stretching/shrinking velocities are described as $v_w(y) = ay\ (y-\text{direction})$ and $u_w(x) = ax\ (x-\text{direction})$, respectively with positive constant a as presented in Fig. 1. Both ambient (T_∞) and wall (T_w) temperatures are constant.

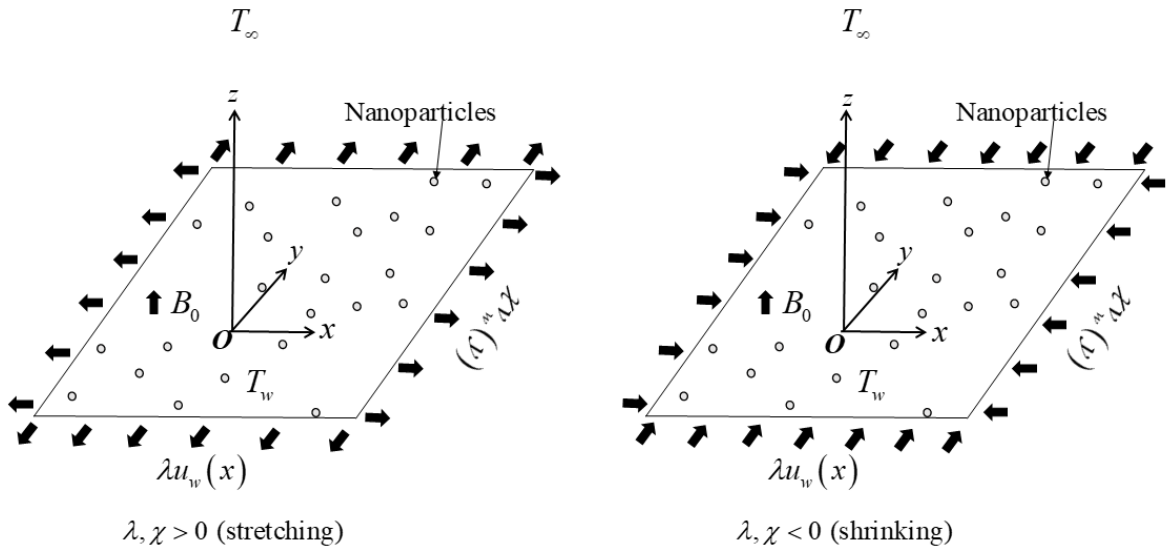

Fig. 1. Physical view of present model

The boundary layer including energy equations are (see Wahid *et al*., [41], Khashi'ie *et al*., [42] and Waini *et al*., [43])

$$\frac{\partial u}{\partial x}+\frac{\partial v}{\partial y}+\frac{\partial w}{\partial z}=0, \tag{1}$$

$$u\frac{\partial u}{\partial x}+v\frac{\partial u}{\partial y}+w\frac{\partial u}{\partial z}=\frac{\mu_{hff}}{\rho_{hff}}\frac{\partial^2 u}{\partial z^2}-\frac{\sigma_{hff}}{\rho_{hff}}B_0^2 u, \tag{2}$$

$$u\frac{\partial v}{\partial x}+v\frac{\partial v}{\partial y}+w\frac{\partial v}{\partial z}=\frac{\mu_{hff}}{\rho_{hff}}\frac{\partial^2 v}{\partial z^2}-\frac{\sigma_{hff}}{\rho_{hff}}B_0^2 v, \tag{3}$$

$$u\frac{\partial T}{\partial x}+v\frac{\partial T}{\partial y}+w\frac{\partial T}{\partial z}=\frac{k_{hff}}{(\rho C_p)_{hff}}\frac{\partial^2 T}{\partial z^2}-\frac{1}{(\rho C_p)_{hff}}\frac{\partial q_r}{\partial z}, \tag{4}$$

with

$$\begin{aligned} &u=\lambda u_w,\quad v=\chi v_w,\quad w=w_w,\quad T=T_w \quad \text{at} \quad z=0\\ &u,v\to 0,\quad T\to T_\infty \quad \text{as} \quad z\to\infty \end{aligned} \tag{5}$$

as the boundary conditions. Here u,v,w are the velocities, T is the fluid temperature, w_w is the mass velocity, λ and χ are the stretching/shrinking parameters. The term q_r in Eq. (6) is approximated using Rosseland formula as

$$q_r = -\frac{4\sigma^*}{3k^*}\frac{\partial T^4}{\partial y}. \tag{6}$$

Using the Taylor series, T^4 in Eq. (6) is simplified as

$$u\frac{\partial T}{\partial x} + v\frac{\partial T}{\partial y} = \left[\frac{k_{hff}}{(\rho C_p)_{hff}} + \frac{16\sigma^* T_\infty^3}{3(\rho C_p)_{hff} k^*}\right]\frac{\partial^2 T}{\partial y^2}. \tag{7}$$

The similarity variables for the similarity solutions are [41,42],

$$u = axf'(\eta), \quad v = ayg'(\eta), \quad w = -\sqrt{a\nu_f}\left[f(\eta)+g(\eta)\right], \quad \theta(\eta) = \frac{T-T_\infty}{T_w - T_\infty}, \quad \eta = z\sqrt{a/\nu_f}. \tag{8}$$

Hence,

$$w_w = -\sqrt{a\nu_f}S \tag{9}$$

where $S > 0$ stands for the suction. The following ODEs are obtained when Eq. (8) is substituted into Eqs. (2), (3) and (7),

$$\frac{\mu_{hff}/\mu_f}{\rho_{hff}/\rho_f}f''' + (f+g)f'' - \left(\frac{\sigma_{hff}/\sigma_f}{\rho_{hff}/\rho_f}M + f'\right)f' = 0, \tag{10}$$

$$\frac{\mu_{hff}/\mu_f}{\rho_{hff}/\rho_f}g''' + (f+g)g'' - \left(\frac{\sigma_{hff}/\sigma_f}{\rho_{hff}/\rho_f}M + g'\right)g' = 0, \tag{11}$$

$$\frac{1}{\Pr}\frac{(\rho C_p)_f}{(\rho C_p)_{hff}}\left(\frac{k_{hff}}{k_f} + \frac{4}{3}R\right)\theta'' + (f+g)\theta' = 0, \tag{12}$$

with the reduced conditions

$$\begin{aligned} &f(0) = S, \quad f'(0) = \lambda, \quad g(0) = 0, \quad g'(0) = \chi, \quad \theta(0) = 1, \\ &f'(\eta) \to 0, \quad g'(\eta) \to 0, \quad \theta(\eta) \to 0 \quad \text{as} \quad \eta \to \infty. \end{aligned} \tag{13}$$

where $\Pr = (C_p\mu)_f / k_f$ (Prandtl number), $M = \sigma_f B_0^2 / \rho_f a$ (magnetic parameter) and $R = 4\sigma^* T_\infty^3 / k_f k^*$ (thermal radiation parameter). Tables 1 and 2 show the correlations and thermophysical properties for hybrid ferrofluids, nanoparticles and base fluid, respectively.

Meanwhile, this definition is essential for the observation of fluid flow behavior and heat transfer characteristics where

$$C_{fx} = \frac{\mu_{hff}/\mu_f}{u_w^2(x)}\left(\frac{\partial u}{\partial z}\right)_{z=0}, \quad C_{fy} = \frac{\mu_{hff}/\mu_f}{v_w^2(y)}\left(\frac{\partial v}{\partial z}\right)_{z=0}, \quad Nu_x = -\frac{xk_{hff}}{k_f(T_w - T_\infty)}\left(\frac{\partial T}{\partial z}\right)_{z=0} + (q_r)_{z=0}. \tag{14}$$

Substituting Eq. (8) into Eq. (14), the reduced coefficients of skin friction and heat transfer are

$$Re_x^{1/2}C_{fx} = \frac{\mu_{hff}}{\mu_f}f''(0), \quad Re_y^{1/2}C_{fy} = \frac{\mu_{hff}}{\mu_f}g''(0), \quad Re_x^{-1/2}Nu_x = -\left(\frac{k_{hff}}{k_f} + \frac{4}{3}R\right)\theta'(0). \tag{15}$$

Table 1
The correlation of a general hybrid nanofluid [41-43]

Properties	Nanofluid
Density	$\rho_{hff} = \phi_1\rho_{s1} + \phi_2\rho_{s2} + \left(1-\phi_{hff}\right)\rho_f$
Heat Capacity	$\left(\rho C_p\right)_{hff} = \phi_1\left(\rho C_p\right)_{s1} + \phi_2\left(\rho C_p\right)_{s2} + \left(1-\phi_{hff}\right)\left(\rho C_p\right)_f$
Dynamic Viscosity	$\mu_{hff} = \frac{\mu_f}{\left(1-\phi_{hff}\right)^{2.5}}; \quad \phi_{hff} = \phi_1 + \phi_2$
Thermal Conductivity	$k_{hff} = \left[\frac{\left(\frac{\phi_1 k_1 + \phi_2 k_2}{\phi_{hff}}\right) - 2\phi_{hff}k_f + 2\left(\phi_1 k_1 + \phi_2 k_2\right) + 2k_f}{\left(\frac{\phi_1 k_1 + \phi_2 k_2}{\phi_{hff}}\right) + \phi_{hff}k_f - \left(\phi_1 k_1 + \phi_2 k_2\right) + 2k_f}\right] k_f$
Electrical Conductivity	$\sigma_{hff} = \left[\frac{\left(\frac{\phi_1 \sigma_1 + \phi_2 \sigma_2}{\phi_{hff}}\right) - 2\phi_{hff}\sigma_f + 2\left(\phi_1 \sigma_1 + \phi_2 \sigma_2\right) + 2\sigma_f}{\left(\frac{\phi_1 \sigma_1 + \phi_2 \sigma_2}{\phi_{hff}}\right) + \phi_{hff}\sigma_f - \left(\phi_1 \sigma_1 + \phi_2 \sigma_2\right) + 2\sigma_f}\right] \sigma_f$

Table 2
Thermophysical properties for $CoFe_2O_4$, Fe_3O_4 and H_2O (see Tlili et al. [32])

Thermophysical Properties	$CoFe_2O_4$	Fe_3O_4	H_2O
C_p(J/kgK)	700	670	4179
ρ (kg/m^3)	4908	5180	997.1
σ (S/m)	1.1 x 10^7	0.74 x 10^6	0.05
k (W/mK)	3.6	9.8	0.6130
Pr	-	-	6.2

3. Stability Analysis

Following Merkin [44] and Weidman *et al.*, [45], the unsteady form of differential equations pertinent to the model were used to discover the stable solution.

$$\frac{\partial u}{\partial t} + u\frac{\partial u}{\partial x} + v\frac{\partial u}{\partial y} + w\frac{\partial u}{\partial z} = \frac{\mu_{hff}}{\rho_{hff}}\frac{\partial^2 u}{\partial z^2} - \frac{\sigma_{hff}}{\rho_{hff}}B_0^2 u, \tag{16}$$

$$\frac{\partial v}{\partial t} + u\frac{\partial v}{\partial x} + v\frac{\partial v}{\partial y} + w\frac{\partial v}{\partial z} = \frac{\mu_{hff}}{\rho_{hff}}\frac{\partial^2 v}{\partial z^2} - \frac{\sigma_{hff}}{\rho_{hff}}B_0^2 v, \tag{17}$$

$$\frac{\partial T}{\partial t} + u\frac{\partial T}{\partial x} + v\frac{\partial T}{\partial y} + w\frac{\partial T}{\partial z} = \left[\frac{k_{hff}}{(\rho C_p)_{hff}} + \frac{16\sigma^* T_\infty^3}{3\,(\rho C_p)_{hff}\,k^*}\right]\frac{\partial^2 T}{\partial z^2} \tag{18}$$

The suitable similarity variables for Eqs. (16)-(18) are [41,42]

$$u = ax\frac{\partial f(\eta,\tau)}{\partial \eta}, \quad v = ay\frac{\partial g(\eta,\tau)}{\partial \eta}, \quad w = -\sqrt{a\nu_f}\left[f(\eta,\tau)+g(\eta,\tau)\right],$$
$$\theta(\eta,\tau) = \frac{T-T_\infty}{T_w-T_\infty}, \quad \eta = z\sqrt{a/\nu_f}. \tag{19}$$

where $\tau = at$ is a time variable. The new differential equations are as follows

$$\left(\frac{\mu_{hff}/\mu_f}{\rho_{hff}/\rho_f}\right)\frac{\partial^3 f}{\partial \eta^3} + (f+g)\frac{\partial^2 f}{\partial \eta^2} - \left(\frac{\sigma_{hff}/\sigma_f}{\rho_{hff}/\rho_f}M + \frac{\partial f}{\partial \eta}\right)\frac{\partial f}{\partial \eta} - \frac{\partial^2 f}{\partial \eta \partial \tau} = 0, \tag{20}$$

$$\left(\frac{\mu_{hff}/\mu_f}{\rho_{hff}/\rho_f}\right)\frac{\partial^3 g}{\partial \eta^3} + (f+g)\frac{\partial^2 g}{\partial \eta^2} - \left(\frac{\sigma_{hff}/\sigma_f}{\rho_{hff}/\rho_f}M + \frac{\partial g}{\partial \eta}\right)\frac{\partial g}{\partial \eta} - \frac{\partial^2 g}{\partial \eta \partial \tau} = 0, \tag{21}$$

$$\frac{1}{\Pr}\frac{(\rho C_p)_f}{(\rho C_p)_{hff}}\left(\frac{k_{hff}}{k_f}+\frac{4}{3}R\right)\frac{\partial^2 \theta}{\partial \eta^2} + (f+g)\frac{\partial \theta}{\partial \eta} - \frac{\partial \theta}{\partial \tau} = 0, \tag{22}$$

with reduced conditions

$$f(0,\tau) = S, \quad \frac{\partial f(0,\tau)}{\partial \eta} = \lambda, \quad g(0,\tau) = 0, \quad \frac{\partial g(0,\tau)}{\partial \eta} = \chi, \quad \theta(0,\tau) = 1,$$
$$\frac{\partial f(\eta,\tau)}{\partial \eta} \to 0, \quad \frac{\partial g(\eta,\tau)}{\partial \eta} \to 0, \quad \theta(\eta,\tau) \to 0 \quad \text{as} \quad \eta \to \infty. \tag{23}$$

For the analysis of stable solution, Eq. (24) (perturbation equation with eigenvalue γ) is substituted in Eqs. (20)-(22). Besides, $F(\eta)$, $G(\eta)$ and $H(\eta)$ are introduced as a relative of $f_0(\eta)$, $g_0(\eta)$ and $\theta_0(\eta)$ accordingly:

$$\left.\begin{aligned} f(\eta,\tau) &= f_0(\eta) + e^{-\gamma\tau}F(\eta) \\ g(\eta,\tau) &= g_0(\eta) + e^{-\gamma\tau}G(\eta) \\ \theta(\eta,\tau) &= \theta_0(\eta) + e^{-\gamma\tau}H(\eta) \end{aligned}\right\} \tag{24}$$

Applying the perturbation equation in (24), Eqs. (20)-(22) are now in the linearized form:

$$\frac{\mu_{hff}/\mu_f}{\rho_{hff}/\rho_f}F''' + (f_0+g_0)F'' - \left(2f_0' - \gamma + \frac{\sigma_{hff}/\sigma_f}{\rho_{hff}/\rho_f}M\right)F' + (F+G)f_0'' = 0, \tag{25}$$

$$\frac{\mu_{hff}/\mu_f}{\rho_{hff}/\rho_f}G''' + (f_0+g_0)G'' - \left(2g_0' - \gamma + \frac{\sigma_{hff}/\sigma_f}{\rho_{hff}/\rho_f}M\right)G' + (F+G)g_0'' = 0, \tag{26}$$

$$\frac{1}{\Pr}\frac{(\rho C_p)_f}{(\rho C_p)_{hff}}\left(\frac{k_{hff}}{k_f}+\frac{4}{3}R\right)H'' + (F+G)\theta_0' + (f_0+g_0)H' + \gamma H = 0, \tag{27}$$

along with the linearized conditions

$$F(\eta)=0,\quad F'(\eta)=0,\quad G(\eta)=0,\quad G'(\eta)=0,\quad H(\eta)=0 \quad \text{at} \quad \eta=0,$$
$$F'(\eta)\to 0,\quad G'(\eta)\to 0,\quad H(\eta)\to 0 \quad \text{as} \quad \eta\to\infty. \tag{28}$$

After linearizing the problem, we now consider $F''(0)=1$ as suggested by Harris et al. [46]. Hence, by solving Eqs. (25)-(28) and replaced $F'(\eta)\to 0$ with the suggested condition, γ_1 is obtained where the solution is stable if the smallest eigenvalues are positive.

4. Results and Discussion

The generation of the similarity solutions in Eqs. (10) to (13) are successfully computed using the bvp4c solver. The impact of physical factors like volumetric concentration of the hybrid nanoparticles, suction, magnetic and radiation parameters are analyzed for the graphical trend of the thermal rate (local Nusselt number) and skin friction coefficients. Meanwhile, the stability analysis are also conducted upon the existence of dual solutions. The available solutions are observed with the consideration of these parameters based on the main references such that $2.5<S\le 3.1$, $0.01\le M\le 0.03$, $0\le \phi_{hff}\le 0.01$ (equal concentration of magnetite and cobalt ferrite) and $0.01\le R\le 0.03$. The equal strength of the stretching/shrinking parameters $(\lambda=\chi)$ is considered except for the validation purpose. The comparison of $-f''(0)$ is done with Wahid et al. [41] and Yusuf et al. [47] as shown in Table 3 which validates the present model. The values of $-\theta'(0)$ are also enclosed for future guidance to the other researchers. For present analysis, two solutions are observed within a certain range of the parameters. Hence, for the justification purpose, stability analysis is conducted as discussed in previous section to analyze the correct solution. Table 4 is designed to compare the smallest eigenvalues between first and second solutions when $\lambda=-1.3$, $\phi_1=\phi_2=0.005$, $R=0.01$, $M=0.02$ and various S. The first solution with positive smallest eigenvalue shows that this solution is the real and stable solution.

Table 3
Validation of the present numerical values $-f''(0)$ when $\lambda=1$, $\chi=0$, $S=\phi_1=\phi_2=0$, $R=0$ and various M

M	$-f''(0)$			$-\theta'(0)$
	Present	Wahid et al. [41]	Yusuf et al. [47]	Present
0	1.000000001	1.000000057	1.000008	1.770947689
1	1.414213562	1.414213562	1.4142143	1.680264667
5	2.449489743	2.449489743	2.4494893	1.457526005
10	3.316624790	3.316624790	3.3166242	1.285700392
50	7.141428429	7.141428429	7.1414285	0.778734625
100	10.049875621	10.049875621	10.049876	0.582228910

Table 4
Smallest eigenvalue from the stability analysis when $\lambda=-1.3,\ \phi_1=\phi_2=0.005,\ R=0.01,\ M=0.02$ and various S

S	γ_1	
	First Solution	Second Solution
2.957	0.6012	-0.0777
2.955	0.3995	-0.0245
2.9549	0.0181	-0.0179
2.9548	0.0063	-0.0063

The effect of suction, shrinking parameter, magnetic and radiation parameters on the reduced $\mathrm{Re}_x^{1/2}C_{fx}$, $\mathrm{Re}_y^{1/2}C_{fy}$ and $\mathrm{Re}_x^{-1/2}Nu_x$ is displayed in Figs. 2-4. In this work, the $\mathrm{Re}_x^{1/2}C_{fx}$, $\mathrm{Re}_y^{1/2}C_{fy}$ and $\mathrm{Re}_x^{-1/2}Nu_x$ are plotted against suction strength S with variation of parameters to further analyze the minimum suction value that is requirable for the acquisition of two solutions. In Figs. 2(a) and 2(b), stronger value of shrinking parameter requires higher value of suction for the generation of two solutions such that $S_3=3.0674\ (\lambda=-1.4),\ S_2=3.0117\ (\lambda=-1.35)$ and $S_1=2.9548\ (\lambda=-1.3)$. Physically, higher shrinking parameter means stronger obstruction for the fluid to flow freely which makes the demand for suction is higher. In addition, both $\mathrm{Re}_x^{1/2}C_{fx}$ and $\mathrm{Re}_x^{-1/2}Nu_x$ increases with the reduction of shrinking parameter $(\lambda=-1.4,-1.35,-1.3)$.Figures 3(a) and 3(b) portrayed the $\mathrm{Re}_x^{-1/2}Nu_x$, $\mathrm{Re}_y^{1/2}C_{fy}$ and $\mathrm{Re}_x^{-1/2}Nu_x$ towards S with different magnetic parameter. The addition of magnetic field reduces the usage of minimum suction strength such that $S_3=2.9621\ (M=0.01)$, $S_2=2.9548\ (M=0.02)$ and $S_1=2.9474\ (\lambda=0.03)$. Further observations show that the magnetic field enhances both skin frictions and thermal rate for each value of S. From physical evaluation, the Lorentz force which evolved from the magnetic field usually opposes the fluid motion (Fe_3O_4-$CoFe_2O_4$/water) and concurrently hold the boundary layer separation [48]. However, in this case, the $\mathrm{Re}_x^{1/2}C_{fx}$ and $\mathrm{Re}_y^{1/2}C_{fy}$ enhances due to the involvement of high suction value $(S>2.9)$.

The visualization of thermal rate and temperature profile with various radiation parameter is presented in Figs. 4(a) and 4(b). Remarkably, the thermal rate deteriorates with the upsurge of R while the minimum suction strength that is necessary to generate all solutions are same for all values of R. This behaviour may happen due to the consideration of shrinking sheet. The radiation parameter only affects the thermal profile of the Fe_3O_4-$CoFe_2O_4$/water due to the process of energy transmission, hence no change in the skin friction coefficients [42]. The addition of R supplies more energy to the Fe_3O_4-$CoFe_2O_4$/water which simultaneously, increase the fluid temperature by thinning the thermal boundary layer as displayed in Fig. 4(b). Besides, it is clear that the temperature profile fulfills the requirement of boundary conditions which affirm the accuracy of present solutions.

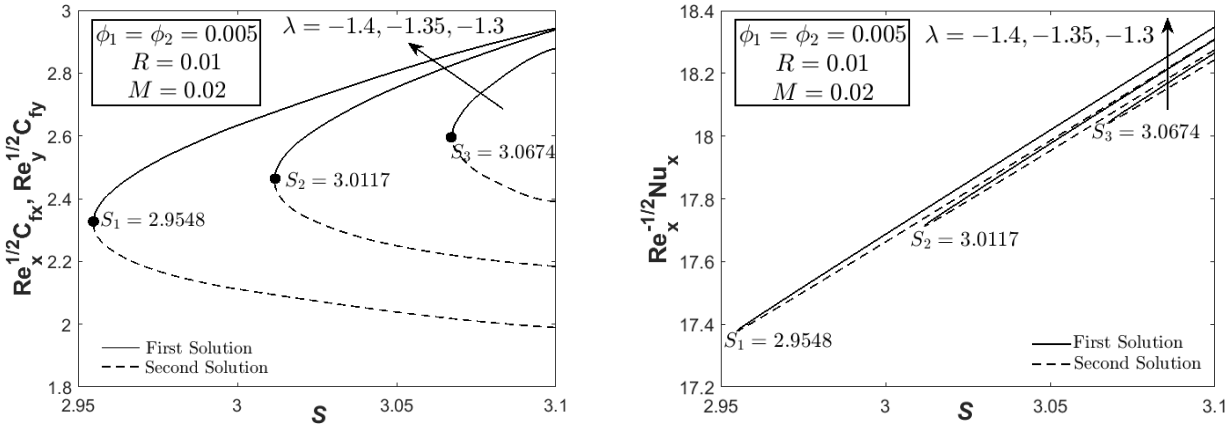

(a) (b)

Fig. 2. (a) Skin friction coefficients, and (b) thermal rate of Fe_3O_4-$CoFe_2O_4$/water towards suction with variation of shrinking parameter

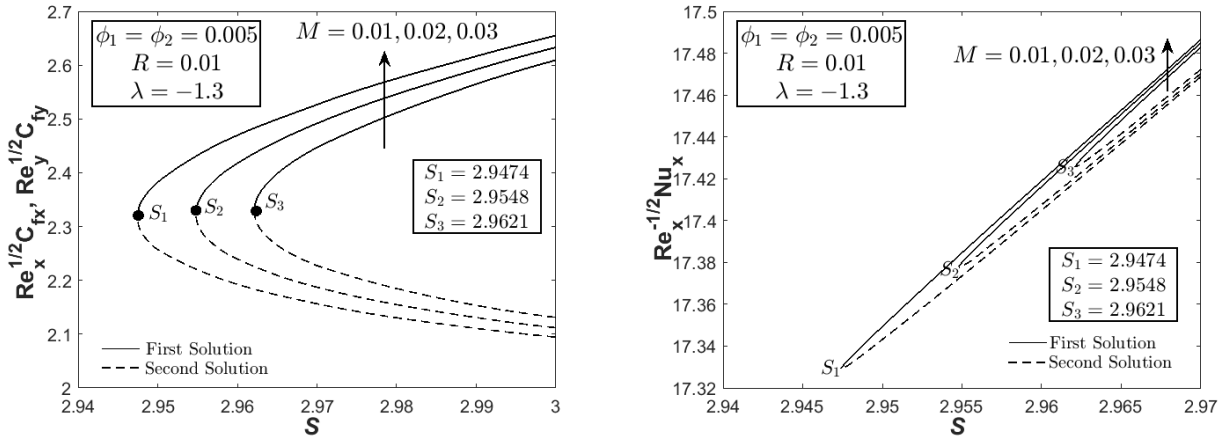

(a) (b)

Fig. 3. (a) Skin friction coefficients, and (b) thermal rate of Fe_3O_4-$CoFe_2O_4$/water towards suction with variation of magnetic strength

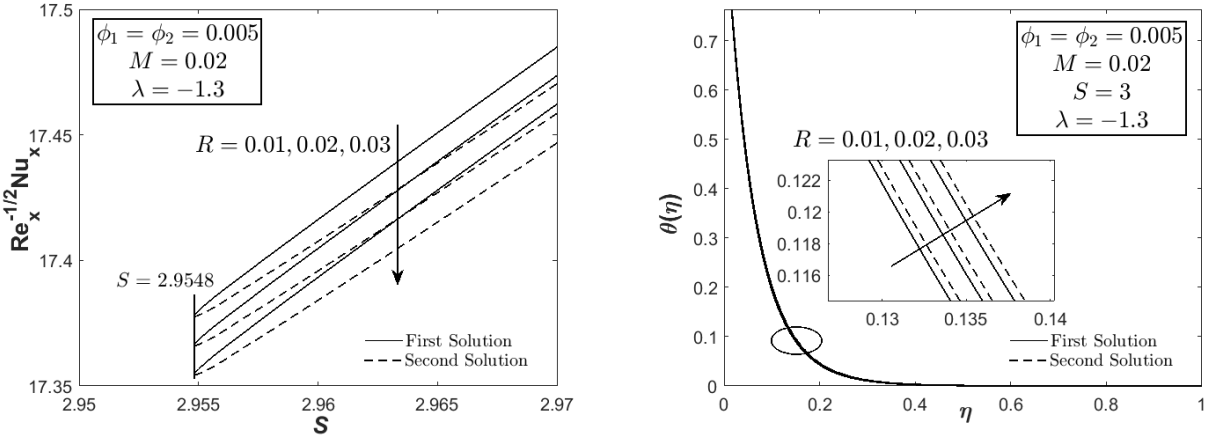

(a) (b)

Fig. 4. (a) Thermal rate, and (b) temperature profile of Fe_3O_4-$CoFe_2O_4$/water with variation of radiation parameter

5. Conclusion

The investigation of the radiative heat flux on the MHD hybrid ferrofluid flow in a three-dimensional system subjected to the shrinking surface is established. The composition of the fluid consists of Fe_3O_4-$CoFe_2O_4$ as the hybrid nanoparticles whereas water is the base fluid. The conclusions can be made from the study are listed as follows:

- Dual solutions are possible for certain values of the physical parameter. This is due to the reverse flow occurs in the boundary layer flow created by the shrinking surface.
- The magnitude of $\mathrm{Re}_x^{1/2} C_{fx}$ and $\mathrm{Re}_x^{-1/2} Nu_x$ are boosted with the imposition of magnetic field on the boundary layer. This behavior occurs due to the resistance force called the Lorentz force which created by the magnetic field.
- However, the present of radiation R is to reduce the $\mathrm{Re}_x^{-1/2} Nu_x$ where the critical point is occurred at the same point. Moreover, the rise of R provides more energy to the fluid which increase the fluid temperature by thinning the thermal boundary layer. Thus, the temperature gradient on the surface is increased and consequently retards the rate of heat transfer.
- The domain of the solutions for S are lessen when the values of λ are increased. This signify that the separation of the boundary layer is fasten for weaker shrinking rate. Similar behavior is observed when larger M is considered.
- By the aids of the temporal stability analysis, the first solution is confirmed to be a stable and relevant solution. Meanwhile, the second solution is unstable. This can be verified from the eigenvalue obtained in the stability analysis where the first solution gives the positive value.

Acknowledgement
We acknowledge the financial support from MOHE Malaysia and Universiti Teknikal Malaysia Melaka through FRGS/1/2021/STG06/UTEM/03/1 (FRGS Scheme).

References

[1] Gudekote, Manjunatha, and Rajashekhar Choudhari. "Slip effects on peristaltic transport of Casson fluid in an inclined elastic tube with porous walls." *Journal of Advanced Research in Fluid Mechanics and Thermal Sciences* 43, no. 1 (2018): 67-80.

[2] Hamrelaine, Salim, Fateh Mebarek-Oudina, and Mohamed Rafik Sari. "Analysis of MHD Jeffery Hamel flow with suction/injection by homotopy analysis method." *Journal of Advanced Research in Fluid Mechanics and Thermal Sciences* 58, no. 2 (2019): 173-186.

[3] Khan, Ansab Azam, Khairy Zaimi, Suliadi Firdaus Sufahani, and Mohammad Ferdows. "MHD flow and heat transfer of double stratified micropolar fluid over a vertical permeable shrinking/stretching sheet with chemical reaction and heat source." *Journal of Advanced Research in Applied Sciences and Engineering Technology* 21, no. 1 (2020): 1-14. https://doi.org/10.37934/araset.21.1.114

[4] Shahrim, Muhammad Nazirul, Ahmad Qushairi Mohamad, Lim Yeou Jiann, Muhamad Najib Zakaria, Sharidan Shafie, Zulkhibri Ismail, and Abdul Rahman Mohd Kasim. "Exact solution of fractional convective Casson fluid through an accelerated plate." *CFD Letters* 13, no. 6 (2021): 15-25. https://doi.org/10.37934/cfdl.13.6.1525

[5] Arifin, Nur Syamilah, Abdul Rahman Mohd Kasim, Syazwani Mohd Zokri, and Mohd Zuki Salleh. "Boundary Layer Flow of Dusty Williamson Fluid with Variable Viscosity Effect Over a Stretching Sheet." *Journal of Advanced Research in Fluid Mechanics and Thermal Sciences* 86, no. 1 (2021): 164-175. https://doi.org/10.37934/arfmts.86.1.164175

[6] Dasman, Anisah, Abdul Rahman Mohd Kasim, Iskandar Waini, and Najiyah Safwa Khashi'ie. "Numerical Solution for Boundary Layer Flow of a Dusty Micropolar Fluid Due to a Stretching Sheet with Constant Wall Temperature." *Journal of Advanced Research in Fluid Mechanics and Thermal Sciences* 87, no. 1 (2021): 30-40. https://doi.org/10.37934/arfmts.87.1.3040

[7] Jamali, Muhammad Sabaruddin Ahmad, Zuhaila Ismail, and Norsarahaida Saidina Amin. "Effect of Different Types of Stenosis on Generalized Power Law Model of Blood Flow in a Bifurcated Artery." *Journal of Advanced Research in Fluid Mechanics and Thermal Sciences* 87, no. 3 (2021): 172-183. https://doi.org/10.37934/arfmts.87.3.172183

[8] Beleri, Joonabi, and Asha S. Kotnurkar. "Peristaltic Transport of Ellis Fluid under the Influence of Viscous Dissipation Through a Non-Uniform Channel by Multi-Step Differential Transformation Method." *Journal of Advanced Research in Numerical Heat Transfer* 9, no. 1 (2022): 1-18.

[9] Mahat, Rahimah, Muhammad Saqib, Imran Ulah, Sharidan Shafie, and Sharena Mohamad Isa. "MHD Mixed Convection of Viscoelastic Nanofluid Flow due to Constant Heat Flux." *Journal of Advanced Research in Numerical Heat Transfer* 9, no. 1 (2022): 19-25.

[10] Zokri, Syazwani Mohd, Nur Syamilah Arifin, Abdul Rahman Mohd Kasim, and Mohd Zuki Salleh. "Flow of jeffrey fluid over a horizontal circular cylinder with suspended nanoparticles and viscous dissipation effect: Buongiorno model." *CFD letters* 12, no. 11 (2020): 1-13. https://doi.org/10.37934/cfdl.12.11.113

[11] Choi, S. US, and Jeffrey A. Eastman. *Enhancing thermal conductivity of fluids with nanoparticles*. No. ANL/MSD/CP-84938; CONF-951135-29. Argonne National Lab.(ANL), Argonne, IL (United States), 1995.

[12] Daungthongsuk, Weerapun, and Somchai Wongwises. "A critical review of convective heat transfer of nanofluids." *Renewable and sustainable energy reviews* 11, no. 5 (2007): 797-817. https://doi.org/10.1016/j.rser.2005.06.005

[13] Ajeeb, Wagd, and SM Sohel Murshed. "Nanofluids in compact heat exchangers for thermal applications: A State-of-the-art review." *Thermal Science and Engineering Progress* (2022): 101276. https://doi.org/10.1016/j.tsep.2022.101276

[14] Mamat, Hussin, and Mohamad Ramadan. "Nanofluids: Thermal Conductivity and Applications." (2022): 288-296. https://doi.org/10.1016/B978-0-12-815732-9.00141-8

[15] Xuan, Lee Wei, Mohd Fadhil Majnis, Syahriza Ismail, and Mohd Azam Mohd Adnan. "Synthesis of bi-component ZrO2/Ag nanotube for heavy metal removal." *Progress in Energy and Environment* 18 (2021): 23-33. https://doi.org/10.37934/progee.18.1.2333

[16] Sharafatmandjoor, Shervin. "Effect of Imposition of viscous and thermal forces on Dynamical Features of Swimming of a Microorganism in nanofluids." *Journal of Advanced Research in Micro and Nano Engineering* 8, no. 1 (2022): 1-8.

[17] Kole, Madhusree, and Sameer Khandekar. "Engineering applications of ferrofluids: A review." *Journal of Magnetism and Magnetic Materials* 537 (2021): 168222. https://doi.org/10.1016/j.jmmm.2021.168222

[18] Horng, Herng-Er, Chin-Yih Hong, Shieh-Yueh Yang, and Hong-Chang Yang. "Novel properties and applications in magnetic fluids." *Journal of Physics and Chemistry of Solids* 62, no. 9-10 (2001): 1749-1764. https://doi.org/10.1016/S0022-3697(01)00108-1

[19] Odenbach, Stefan. "Ferrofluids and their applications." *MRS bulletin* 38, no. 11 (2013): 921-924. https://doi.org/10.1557/mrs.2013.232

[20] Babu, JA Ranga, K. Kiran Kumar, and S. Srinivasa Rao. "State-of-art review on hybrid nanofluids." *Renewable and Sustainable Energy Reviews* 77 (2017): 551-565. https://doi.org/10.1016/j.rser.2017.04.040

[21] Sundar, L. Syam, Manoj K. Singh, and Antonio CM Sousa. "Enhanced heat transfer and friction factor of MWCNT–Fe3O4/water hybrid nanofluids." *International Communications in Heat and Mass Transfer* 52 (2014): 73-83. https://doi.org/10.1016/j.icheatmasstransfer.2014.01.012

[22] Abbas, Farrukh, Hafiz Muhammad Ali, Muhammad Shaban, Muhammad Mansoor Janjua, Tayyab Raza Shah, Mohammad Hossein Doranehgard, Majid Ahmadlouydarab, and Farukh Farukh. "Towards convective heat transfer optimization in aluminum tube automotive radiators: Potential assessment of novel Fe2O3-TiO2/water hybrid nanofluid." *Journal of the Taiwan Institute of Chemical Engineers* 124 (2021): 424-436. https://doi.org/10.1016/j.jtice.2021.02.002

[23] Mishra, Ashish, and Himanshu Upreti. "A comparative study of Ag–MgO/water and Fe3O4–CoFe2O4/EG–water hybrid nanofluid flow over a curved surface with chemical reaction using Buongiorno model." *Partial Differential Equations in Applied Mathematics* 5 (2022): 100322. https://doi.org/10.1016/j.padiff.2022.100322

[24] Izady, Mohammad, Saeed Dinarvand, Ioan Pop, and Ali J. Chamkha. "Flow of aqueous Fe2O3–CuO hybrid nanofluid over a permeable stretching/shrinking wedge: A development on Falkner–Skan problem." *Chinese Journal of Physics* 74 (2021): 406-420. https://doi.org/10.1016/j.cjph.2021.10.018

[25] Elsaid, Essam M., and Mohamed S. Abdel-wahed. "MHD mixed convection Ferro Fe3O4/Cu-hybrid-nanofluid runs in a vertical channel." *Chinese Journal of Physics* 76 (2022): 269-282. https://doi.org/10.1016/j.cjph.2021.12.016

[26] Khazayinejad, Mehdi, and S. S. Nourazar. "On the effect of spatial fractional heat conduction in MHD boundary layer flow using Gr-Fe3O4–H2O hybrid nanofluid." *International Journal of Thermal Sciences* 172 (2022): 107265. https://doi.org/10.1016/j.ijthermalsci.2021.107265

[27] Nabwey, Hossam A., and A. Mahdy. "Transient flow of micropolar dusty hybrid nanofluid loaded with Fe3O4-Ag nanoparticles through a porous stretching sheet." *Results in Physics* 21 (2021): 103777. https://doi.org/10.1016/j.rinp.2020.103777

[28] Khan, M. Ijaz, Sumaira Qayyum, Faisal Shah, R. Naveen Kumar, RJ Punith Gowda, B. C. Prasannakumara, Yu-Ming Chu, and S. Kadry. "Marangoni convective flow of hybrid nanofluid (MnZnFe2O4-NiZnFe2O4-H2O) with Darcy Forchheimer medium." *Ain Shams Engineering Journal* 12, no. 4 (2021): 3931-3938. https://doi.org/10.1016/j.asej.2021.01.028

[29] Li, Yi-Xia, Sumaira Qayyum, M. Ijaz Khan, Yasser Elmasry, and Yu-Ming Chu. "Motion of hybrid nanofluid (MnZnFe2O4–NiZnFe2O4–H2O) with homogeneous–heterogeneous reaction: Marangoni convection." *Mathematics and Computers in Simulation* 190 (2021): 1379-1391. https://doi.org/10.1016/j.matcom.2021.07.017

[30] Anuar, Nur Syazana, Norfifah Bachok, and Ioan Pop. "Influence of MHD Hybrid Ferrofluid Flow on Exponentially Stretching/Shrinking Surface with Heat Source/Sink under Stagnation Point Region." *Mathematics* 9, no. 22 (2021): 2932. https://doi.org/10.3390/math9222932

[31] Hosseinzadeh, Kh, So Roghani, A. Asadi, Amirreza Mogharrebi, and D. D. Ganji. "Investigation of micropolar hybrid ferrofluid flow over a vertical plate by considering various base fluid and nanoparticle shape factor." *International Journal of Numerical Methods for Heat & Fluid Flow* 31, no. 1 (2020): 402-417. https://doi.org/10.1108/HFF-02-2020-0095

[32] Tlili, Iskander, M. T. Mustafa, K. Anantha Kumar, and N. Sandeep. "Effect of asymmetrical heat rise/fall on the film flow of magnetohydrodynamic hybrid ferrofluid." *Scientific reports* 10, no. 1 (2020): 1-11. https://doi.org/10.1038/s41598-020-63708-y

[33] Rosseland, Svein. *Astrophysik: Auf atomtheoretischer grundlage*. Vol. 11. Springer-Verlag, 2013.

[34] Sparrow, E. M., and R. D. Cess. "Radiation Heat Transfer, Augmented edition, Hemisphere Publ." *Crop., Washington, DC* (1978).

[35] Yaseen, Moh, Manoj Kumar, and Sawan Kumar Rawat. "Assisting and opposing flow of a MHD hybrid nanofluid flow past a permeable moving surface with heat source/sink and thermal radiation." *Partial Differential Equations in Applied Mathematics* 4 (2021): 100168. https://doi.org/10.1016/j.padiff.2021.100168

[36] Gumber, Priya, Moh Yaseen, Sawan Kumar Rawat, and Manoj Kumar. "Heat transfer in micropolar hybrid nanofluid flow past a vertical plate in the presence of thermal radiation and suction/injection effects." *Partial Differential Equations in Applied Mathematics* 5 (2022): 100240. https://doi.org/10.1016/j.padiff.2021.100240

[37] Rana, Puneet, Saloni Gupta, and Gaurav Gupta. "Unsteady nonlinear thermal convection flow of MWCNT-MgO/EG hybrid nanofluid in the stagnation-point region of a rotating sphere with quadratic thermal radiation: RSM for optimization." *International Communications in Heat and Mass Transfer* 134 (2022): 106025. https://doi.org/10.1016/j.icheatmasstransfer.2022.106025

[38] Bakar, Shahirah Abu, Norihan Md Arifin, Norfifah Bachok, and Fadzilah Md Ali. "Effect of thermal radiation and MHD on hybrid Ag–TiO2/H2O nanofluid past a permeable porous medium with heat generation." *Case Studies in Thermal Engineering* 28 (2021): 101681. https://doi.org/10.1016/j.csite.2021.101681

[39] Mahabaleshwar, U. S., A. B. Vishalakshi, and Helge I. Andersson. "Hybrid nanofluid flow past a stretching/shrinking sheet with thermal radiation and mass transpiration." *Chinese Journal of Physics* 75 (2022): 152-168. https://doi.org/10.1016/j.cjph.2021.12.014

[40] Shoaib, Muhammad, Muhammad Asif Zahoor Raja, Muhammad Touseef Sabir, Muhammad Awais, Saeed Islam, Zahir Shah, and Poom Kumam. "Numerical analysis of 3-D MHD hybrid nanofluid over a rotational disk in presence of thermal radiation with Joule heating and viscous dissipation effects using Lobatto IIIA technique." *Alexandria Engineering Journal* 60, no. 4 (2021): 3605-3619. https://doi.org/10.1016/j.aej.2021.02.015

[41] Syahirah Wahid, Nur, Norihan Md Arifin, Najiyah Safwa Khashi'ie, Ioan Pop, Norfifah Bachok, and Mohd Ezad Hafidz Hafidzuddin. "Three-Dimensional Stretching/Shrinking Flow of Hybrid Nanofluid with Slips and Joule Heating." *Journal of Thermophysics and Heat Transfer* (2022): 1-10. https://doi.org/10.2514/1.T6488

[42] Khashi'ie, Najiyah S., Nur S. Wahid, Norihan Md Arifin, and Ioan Pop. "Insight into three-dimensional flow of three different dynamics of nanofluids subject to thermal radiation: The case of water–cobalt ferrite, water–manganese–zinc ferrite, and water–magnetite." *Heat Transfer* (2022). https://doi.org/10.1002/htj.22506

[43] Waini, Iskandar, Najiyah Safwa Khashi'ie, Abdul Rahman Mohd Kasim, Nurul Amira Zainal, Khairum Bin Hamzah, Norihan Md Arifin, and Ioan Pop. "Unsteady Magnetohydrodynamics (MHD) Flow of Hybrid Ferrofluid Due to a Rotating Disk." *Mathematics* 10, no. 10 (2022): 1658. https://doi.org/10.3390/math10101658

[44] Merkin, J. H. "On dual solutions occurring in mixed convection in a porous medium." *Journal of engineering Mathematics* 20, no. 2 (1986): 171-179. https://doi.org/10.1007/BF00042775

[45] Weidman, P. D., D. G. Kubitschek, and A. M. J. Davis. "The effect of transpiration on self-similar boundary layer flow over moving surfaces." *International journal of engineering science* 44, no. 11-12 (2006): 730-737. https://doi.org/10.1016/j.ijengsci.2006.04.005

[46] Harris, S. D., D. B. Ingham, and I. Pop. "Mixed convection boundary-layer flow near the stagnation point on a vertical surface in a porous medium: Brinkman model with slip." *Transport in Porous Media* 77, no. 2 (2009): 267-285. https://doi.org/10.1007/s11242-008-9309-6

[47] Yusuf, T. A., F. Mabood, W. A. Khan, and J. A. Gbadeyan. "Irreversibility analysis of Cu-TiO2-H2O hybrid-nanofluid impinging on a 3-D stretching sheet in a porous medium with nonlinear radiation: Darcy-Forchhiemer's model." *Alexandria Engineering Journal* 59, no. 6 (2020): 5247-5261. https://doi.org/10.1016/j.aej.2020.09.053

[48] Khashi'ie, Najiyah Safwa, Nur Syahirah Wahid, Norihan Md Arifin, and Ioan Pop. "Magnetohydrodynamics unsteady separated stagnation-point (USSP) flow of a hybrid nanofluid on a moving plate." *ZAMM-Journal of Applied Mathematics and Mechanics/Zeitschrift für Angewandte Mathematik und Mechanik* (2022): e202100410. https://doi.org/10.1002/zamm.202100410